NJC

# Self-assembly synthesis of Co3O4/ multi walled carbon nanotubes composites: An efficient enzyme-free glucose sensor



| | |
|---|---|
| Journal: | *New Journal of Chemistry* |
| Manuscript ID | NJ-ART-06-2015-001447.R1 |
| Article Type: | Paper |
| Date Submitted by the Author: | 07-Sep-2015 |
| Complete List of Authors: | Bhat, Badekai Ramachandra; National Institute of Technology Karnataka, Surathkal, Chemistry<br>Prasad, Raghavendra; National Institute of Technology Karnataka, Surathka, Chemistry |
| | |

Journal Name

ARTICLE

# Self-assembly synthesis of $Co_3O_4$/ multi walled carbon nanotubes composites: An efficient enzyme-free glucose sensor

Received 00th January 20xx,
Accepted 00th January 20xx

DOI: 10.1039/x0xx00000x

www.rsc.org/

Raghavendra Prasad,[a] and Badekai Ramachandra Bhat [a*+]

Self-assembling cobalt oxide-multiwall carbon nanotube composites were synthesized by simple and effective wet chemical routes. Using this material, the modified glassy carbon electrode was fabricated and investigated for enzyme-free glucose sensor application. The fabricated sensor exhibited high sensitivity of 5089.1 μA $mM^{-1}$ $cm^{-2}$ with the detection limit of 10.42 μM over a glucose concentration ranging from 0.05-12 mM. The sensor also shows a promising sensor features like stability, selectivity and fast detection. Moreover, the detection of glucose in human blood serum samples with the as-developed sensor agreed well with the results obtained from commercial glucose meters.

## Introduction

Over the past two decades, major efforts have been devoted for the development of possible alternative material for the electrochemical detection of glucose such as carbon nanotube (CNT), graphene, conducting polymers, etc.[1-3] Among carbon materials, CNT is considered to be a potentially promising candidate because of its low cost, good conductivity, easily functionalized properties, large surface areas and excellent corrosion resistance in various electrolytes.[4,5] Ever since its discovery, because of the special structural, mechanical, electronic and fast electron transfer properties, the CNTs have gained substantial attention in electronic applications.[6-8] Many researchers around the world have focused on the development of CNT decoration with metal and metal-oxide nanoparticles (NPs) to obtain the active components for the non-enzymatic glucose sensor such as NiO, CuO, $Co_3O_4$ and $MnO_2$ etc.[9–16] Generally these metal oxide based sensors direct electro oxidise the glucose mediating by $M^{2+}/M^{3+}$ (M= metal) in alkaline medium. Taking the advantages of simplicity, reproducibility and stability in aggressive environment more and more attention has been provided for metal-oxide based non-enzymatic glucose sensing.[8-12] However, only few have reported on the glucose sensor based on $Co_3O_4$. Due to its low cost, high chemical stability and reasonably high specific capacitance, has been widely studied and documented in the energy and biosensor research, such as supercapacitor, biosensors and lithium-ion cathode materials.[17–22] As an important transition element, cobalt and its oxides have shown excellent sensing properties over a wide range of glucose concentrations.[13,14,19,20] However, due to the large surface area and greater ability to promote electron-transfer ability of the CNT, the composites of $Co_3O_4$ and MWCNT are mainly used in sensor fabrication. Many methods were reported for the synthesis of $Co_3O_4$-MWCNTs nanocomposites.[17,23–26] However, these methods are associated with high cost, complicated as well as uniform decorations of nanoparticles remains a greater challenge. Therefore, a facile and cost-effective method for the large scale synthesis of uniform decorated $Co_3O_4$-MWCNTs composites is a challenge and very active research area.

At the same time, diabetes is one of the major health concerns, which constitutes about 5 % of the world's population ,[27] hence continuous monitoring of human blood sugar level has attained remarkable attention. However, glucose oxidase (GOx) enzyme based sensor played a leading role in the blood sugar monitoring.[28–31] Even though the enzyme based sensor has good selectivity and high sensitivity, it is associated with the most

common and serious limitations to environmental aspects such as temperature, humidity, pH and chemical reagents, resulting in damage to enzymes which leads to lack of long-term stability.[32–34] To overcome these limitations, the enzyme-free glucose sensors have been explored. The enzyme-free detection of glucose is associated with several advantages such as fabrication and storage conditions that are cheap and simple, no enzyme denaturation and degradation and the sensors have more stability towards higher temperatures, pH and more resistance to toxic chemicals which could reduce the working performance of enzyme-based glucose sensors.[35,36]

Herein, we report self-assembled uniform decoration of $Co_3O_4$-NPs on the surface of MWCNT by simple wet chemical routes. Poly (ethylene glycol) (PEG) was used as a capping agent to control the $Co_3O_4$ size and average diameter of 6.7 nm was achieved. Utilising the advantage of large surface area, high electronic conductivity of MWCNT and high catalytic activity of cobalt, the $Co_3O_4$-MWCNT composite samples are explored for the possible electrochemical enzyme-free glucose sensor application. The sensor parameters like optimised operating potential, sensitivity, limit of detection (LOD), selectivity and stability of the sensor were systematically investigated and compared with the reported nanomaterial based enzyme-free glucose sensors.

## Experimental

### Chemicals and reagents

Cobalt (II) acetate tetrahydrate, poly(ethylene glycol) 8000 (PEG) ($M_w$ = 7000-9000), D-(+)-glucose, D-(−)-fructose, D-(+)-maltose monohydrate, sucrose, L-ascorbic acid (AA), uric acid (UA), dopamine hydrochloride (DA) and N,N-dimethylformamide (DMF) were obtained from Sigma-Aldrich and were used as received. All reagents were of analytical grade. All solutions were prepared with high quality deionized water (18.4 MΩ $cm^{-1}$). The Human blood serum (HBS) samples were voluntarily given by the patients for conducting the experiments and study protocol was approved by the Institutional review board at National Institute of Technology Karnataka. Patients gave voluntary written informed consent before their participation. The MWCNTs were synthesized, purified and functionalised using the reported procedure from our research group.[37] Briefly, MWCNTs synthesis was carried out in horizontal tubular furnace at atmospheric pressure. The 300 mg of nickel formate catalyst precursor with $CaCO_3$ support was taken in quartz boat, which was placed in the centre of the quartz tube. Initially argon gas was used to purge the reactor while furnace was heated to 700 °C in 10 min. The CNTs were synthesized by passing the reaction mixture containing acetylene (20 standard cubic centimeters per minute (sccm)) and argon (200 sccm) gas in the ratio 1:10 for 15 min. After the growth the reaction chamber was cooled down slowly to room temperature and black amorphous carbon as a crude product was obtained. To purify the sample, the crude product was first heated under air atmosphere at 380 °C for 2 h to remove amorphous carbon and then stirred in dilute HCl to remove catalyst and $CaCO_3$ support. Finally, the sample was rinsed with distilled water to remove traces of acid.

### Instruments

Autolab PGSTAT30 (Eco Chemie) electrochemical workstation driven by NOVA 1.9 software was used to collect electrochemical data (www.metrohm-autolab.com). A conventional three-electrode cell assembly was used. The $Co_3O_4$-MWCNT nanocomposite modified glassy carbon electrode (GCE) was used as the working electrode. Standard calomel electrode and platinum wire were used as reference and counter electrodes, respectively. All the measurements were carried out at room temperature. The X-ray diffraction (XRD) patterns of the products were determined by Philips X-ray diffractometer using Cu Kα radiation. The morphologies of the nanostructures were observed by JEOL JSM-6400F field emission scanning electron microscope (FESEM). Transmission electron microscopy (TEM) (JEOL-3010F). Raman spectra were recorded at room temperature with laser excitation wavelength of 532 nm.

### Preparation of $Co_3O_4$ /MWCNTs composites

Self-assembly uniform decoration of $Co_3O_4$ on MWCNT was achieved by simple wet chemical method. The MWCNTs (20 mg), was taken in a solution of 20 mL of DMF consist of cobalt (II) acetate tetrahydrate (10 mg) and PEG (10 mg). The weight ratio of MWCNT and cobalt precursor was maintained to be (2:1) and the PEG was used as a capping agent. The above suspension was ultrasonicated for 30 min for uniform dispersion and later further ultra-sonicated in glycerol bath at 125 °C until the solution gets evaporated. The residue obtained was subjected to the thermal treatment at 400 °C for 15 min under an ambient atmosphere. The product was collected as black powder and stored for

characterization and electrode fabrication. For comparison studies, pure $Co_3O_4$ was synthesized similarly.

**Electrode fabrication**

GCE (∅= 4.0 mm ) was polished with 0.3 µm and 0.05 µm alumina slurries, respectively to obtain a mirror-like surface and was then ultrasonically cleaned in ethanol and water successively. After these pre-treatments, the electrode was allowed to dry at room temperature. For preparation of $Co_3O_4$/MWCNTs modified electrodes, 5 mg $Co_3O_4$/MWCNT composite and 1 mL of 0.5 wt% Nafion solution were mixed ultrasonically. Then resulting suspensions (5.0 µL) was drop casted onto the GCE surface and allowed to dry prior to use. For comparison studies, the $Co_3O_4$/GCE and MWCNT/GCE was prepared under identical conditions

## Results and discussion

**Morphologies and structural characterization**

The $Co_3O_4$ NPs decorated MWCNT were prepared by above mentioned wet-chemical method. The structure, morphology, electrochemical properties towards direct glucose oxidation was proposed. The cobalt is expected to electro catalyse the glucose where, the MWCNT acts as a transducer and provides fast electron movement and expecting to enhances the electronic signals.

The surface morphology of the synthesized $Co_3O_4$/MWCNT composite was characterized using FESEM and TEM analysis. An overview of FESEM and TEM micrographs of pure MWCNT, $Co_3O_4$ and $Co_3O_4$/MWCNT composite are shown in the Fig. 1a-e. The FESEM micrographs of pure MWCNT (Fig. 1a), appears like a mesh, on which $Co_3O_4$ NPs was decorated using sol-gel method, these $Co_3O_4$-NPs are wrapping around the MWCNTs (Fig. 1b). $Co_3O_4$-NPs synthesized using similar method which appears to be granular particles in nature (Fig. 1c). The TEM micrograph of MWCNT (Fig. 1d) shows that average diameter of about 8.09 nm (Fig. S1a, Supplementary Information,(SI)) and length of few microns. However, in the composite sample, the TEM micrograph (Fig. 1e) shows average size of about 2.9 nm (Fig. S1b, SI), dark spherical stain on the surface of the MWCNT, which are attributed to the self-assembled $Co_3O_4$-NPs on the surface of MWCNTs (Fig. S2, SI). TEM micrograph of $Co_3O_4$-NPs synthesized appears to be granular in shape with average size of about 6.7 nm (Fig. S1c, SI), which clearly suggested the formation of the $Co_3O_4$-NPs. Hence, from the morphology studies it can be concluded that $Co_3O_4$-NPs were uniformly decorated on the surface of the MWCNT.

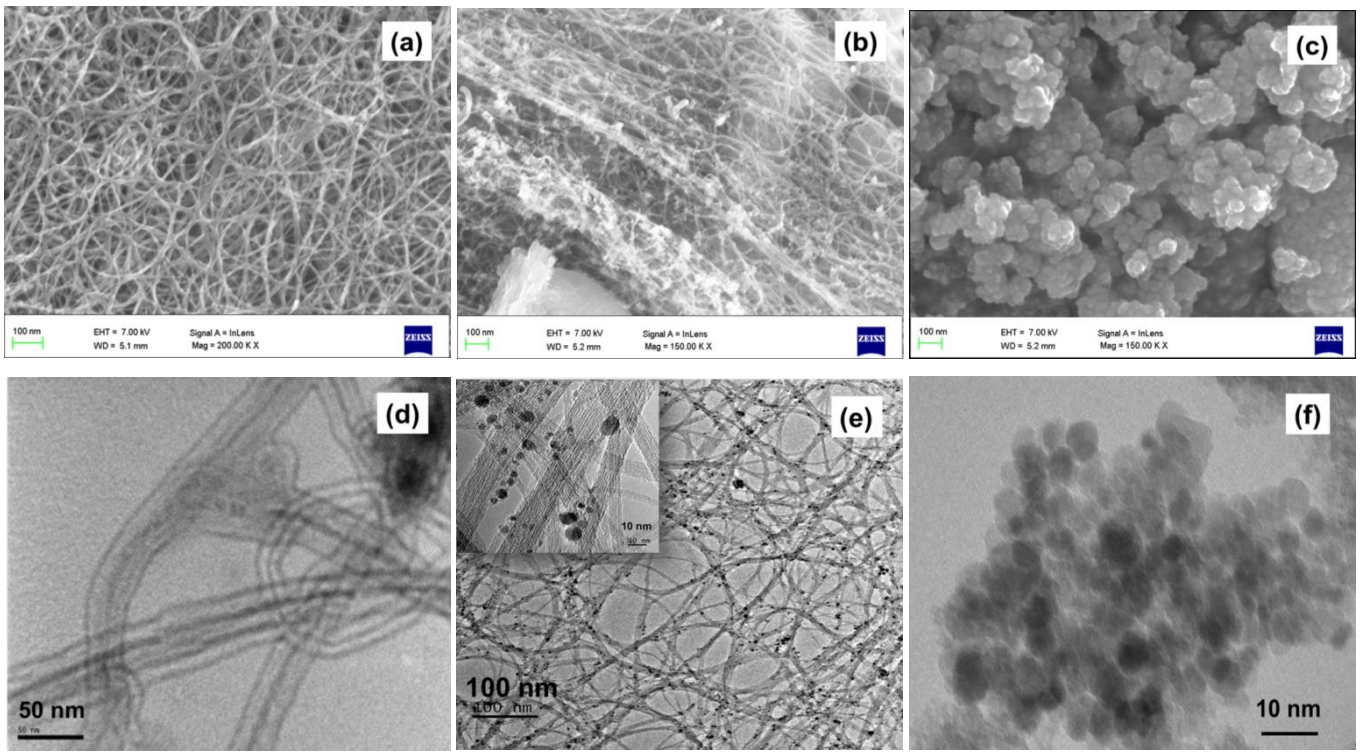


Fig.1. FESEM images of (a) pure MWCNT, (b) $Co_3O_4$-MWCNT composite, (c) $Co_3O_4$ NPs and TEM images of (d) pure MWCNT, (e) $Co_3O_4$-MWCNT composite (with higher magnification inset) and (f) $Co_3O_4$ NPs.

Journal Name

ARTICLE

The samples were further examined by XRD and the results are shown in the Fig. 2a. These results exhibit different diffraction peaks associated with MWCNT and $Co_3O_4$. The diffraction pattern of $Co_3O_4$-MWCNT shows the characteristic peaks of cubic $Co_3O_4$ and the peaks at 18.9°, 31.2°, 36.83°, 38.5°, 44.8°, 55.6°, 59.3° and 65.2° corresponding to (111), (220), (311), (222), (400), (422), (511) and (440) crystal planes (JCPDS no. 009-0148) along with diffraction peak at 26.3° representing (002) crystal plane of MWCNTs. However, decrease in relative intensity of the $Co_3O_4$ diffraction peaks in composite sample is due to the amorphous nature of the MWCNTs. These results suggest the obtained product by sol-gel self-assembly process is a mixture of $Co_3O_4$ and MWCNT and there were no other peaks in the spectrum indicating the high purity of sample. Raman spectra of $Co_3O_4$-MWCNT hybrid was examined for the further evidence of successful assembly of the Co on MWCNT. The Fig. 2b shows Raman spectra of the synthesized samples. The peaks at ~1337 $cm^{-1}$ and ~1586 $cm^{-1}$ are the two characteristic peaks for the MWCNTs. The former is the D band which is ascribed to the glassy carbon or disordered graphite and the latter G-band corresponds to the vibrations of $sp^2$ bonded carbon atoms of two-dimensional hexagonal lattice in graphite.[37,38] The $I_D/I_G$ ratio was effectively used to evaluate the degree of disorder in the sample, increase in $I_D/I_G$ ratio from 0.81 to 1.21 for MWCNT and $Co_3O_4$-MWCNT was observed, this suggests the defects introduced in the composite sample due to the destructive interaction of Co with the MWCNT. In fact, the composite spectrum also shows the three other peaks at 483 $cm^{-1}$, 525 $cm^{-1}$ and 694 $cm^{-1}$ which are attributed to the $Co_3O_4$ which matches well with the spectrum recorded for pure $Co_3O_4$.[39, 40]

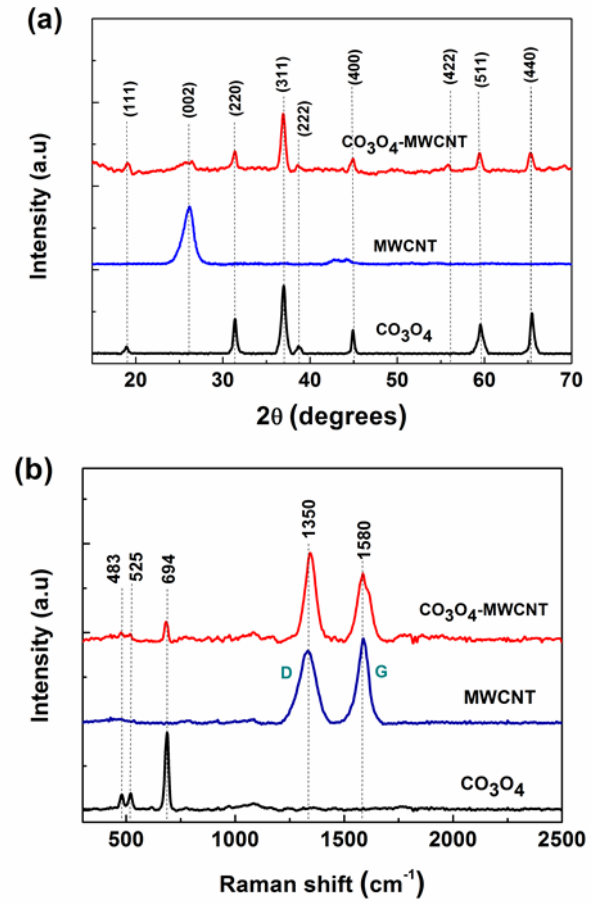


Fig. 2. (a) XRD spectra and (b) Raman spectra of $Co_3O_4$ NPs, pure MWCNTs and $Co_3O_4$/MWCNT nanocomposites.

**Electrochemical behaviour of the $Co_3O_4$/MWCNT/GCE**

The CVs of the $Co_3O_4$/GCE and $Co_3O_4$/MWCNT/GCE composite samples were investigated for the direct oxidation of glucose in both alkaline solution (0.2 M NaOH) and neutral phosphate buffer solution (0.1 M, pH 7.0) in the range from −0.4 V to 0.7 V (Fig. 3a). There was no oxidation or reduction peak seen in the phosphate buffer solution (inset Fig. 3a), while two pairs of well-defined redox peaks were obtained in NaOH solution. This redox peaks formed suggests that the $OH^-$ participates in the electrochemical redox reaction of $Co_3O_4$. From the Fig 3b, as labelled pair of redox peaks I/II can be ascribed to the reversible transformation between $Co_3O_4$ and CoOOH while another pair of redox peaks III/IV can be

assigned to further transition between CoOOH and $CoO_2$.[13,14,20] These two reversible redox reactions can be illustrated as in Eqs. (1) and (2):

$$Co_3O_4 + OH^- + H_2O \rightleftharpoons 3CoOOH + e^- \quad \ldots\ldots\ldots(1)$$

$$CoOOH + OH^- \rightleftharpoons CoO_2 + H_2O + e^- \quad \ldots\ldots\ldots\ldots\ldots(2)$$

The direct catalytic oxidation of glucose at the $Co_3O_4$/GCE and $Co_3O_4$/MWCNT/GCE was first examined in 0.2 M NaOH. The Fig. 3b presents the CVs in the absence and presence of 2 mM glucose of $Co_3O_4$/GCE (curve a and c) and the $Co_3O_4$/MWCNT/GCE (curves b and d), respectively. The $Co_3O_4$/GCE and $Co_3O_4$/MWCNT/GCE exhibited oxidation peak for glucose starting at +0.25 and +0.20 V, respectively and covering the potential region where CoOOH and $CoO_2$ are formed. These results suggest that the direct catalytic oxidation of glucose in 0.2 M NaOH solution was referred to CoOOH and $CoO_2$. From the Fig. 3b it also observed that with the addition of glucose, $Co_3O_4$-MWCNT/GCE shows notable increase in the redox peak current but negligible in case of $Co_3O_4$/GCE, which can be attributed to the synergistic effect of $Co_3O_4$ and MWCNT make the substrate a better platform for electron transfer between $Co_3O_4$ NPs and GCE. This increase in current with increased glucose concentration attributes to the direct catalytic activity of the $Co_3O_4$/MWCNT toward glucose. In addition, peak iii (CoOOH → $CoO_2$) which causes the electro-oxidation of glucose is mainly mediated in a NaOH solution hence the peak iii potential was applied for subsequent amperometric detection. It is also well known that glucose can be oxidized to produce gluconolactone through 2-electron electrochemical reaction.[19] Therefore the possible mechanism of glucose electrochemical oxidation reaction catalyzed by $Co_3O_4$ at peak iii (+0.55 V) can be illustrated as following Eq. 3.

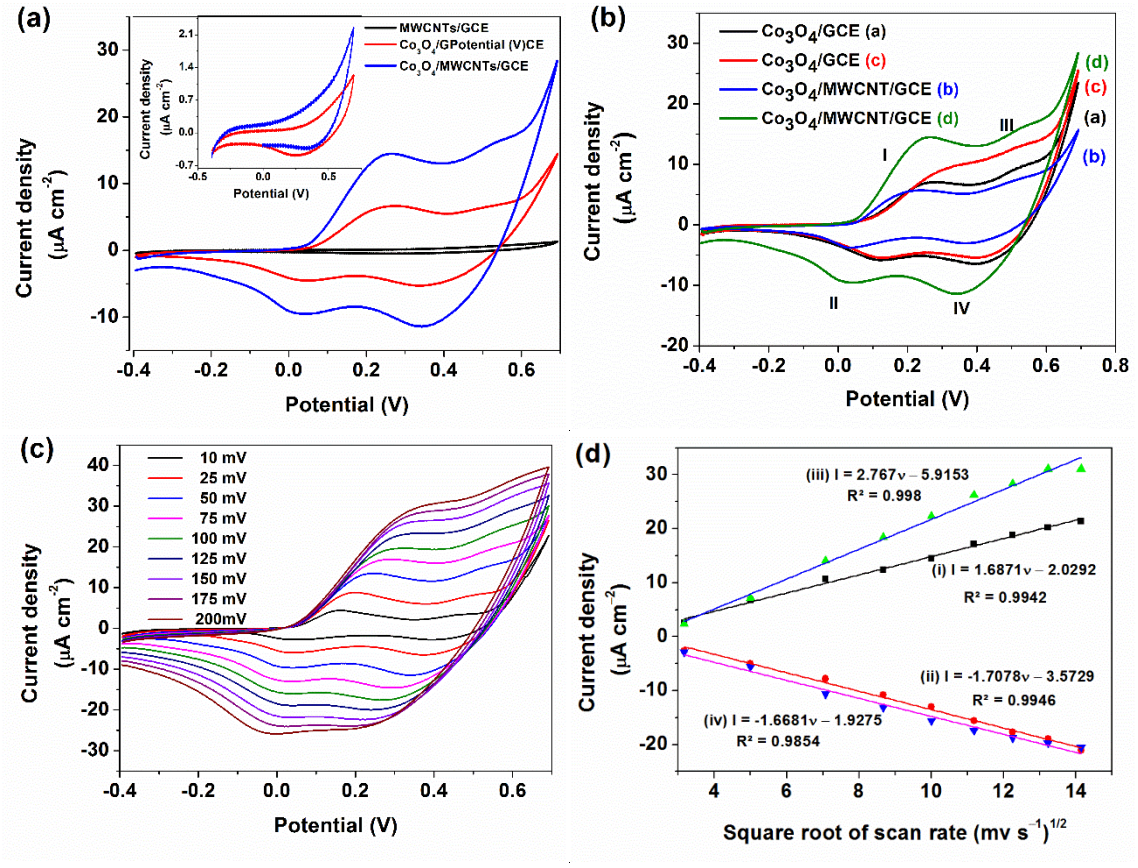


Fig. 3 (a) Cyclic voltammograms of $Co_3O_4$/GCE and $Co_3O_4$/MWCNT/GCE in the 0.2 M NaOH and 0.1 M phosphate buffer solution (inset Fig. 3a), (b) Cyclic voltammograms of $Co_3O_4$/GCE and $Co_3O_4$/MWCNT/GCE in the absence (a, b) and presence, (c, d) of 2.0 mM glucose in 0.2 M NaOH. Scan rate: 50 mV $s^{-1}$, (c) Cyclic voltammograms of $Co_3O_4$/MWCNT/GCE at different scan rates from 10 mV $s^{-1}$ to 200 mV $s^{-1}$ in 0.2 M NaOH with 2.0 mM glucose and (d) plot of peak current density vs. square root of scan rate.

$2CoO_2 + C_6H_{12}O_6\,(glucose) \rightarrow$

$2CoOOH + C_6H_{10}O_6\,(gluconolactone)$ ..... (3)

The information about electrochemical mechanism can be obtained from the relation between peak current and scan rate potential. Hence the effect of scan rate on electro oxidation of glucose on $Co_3O_4$/MWCNT/GCE was also investigated. The Fig. 3c shows the cyclic voltammograms of $Co_3O_4$/MWCNT/GCE with 2 mM glucose at different scan rates ranging from 10 to 200 mV $s^{-1}$. From the obtained results it is observed that anodic and cathodic peak currents increased with increasing scan rate. From the Fig. 3d the anodic and cathodic peak currents are linearly correlated to the square root of scan rate (mV $s^{-1})^{1/2}$ and the corresponding linear regression equations with the linear correlation coefficient values are as follows

(i) $I_{pa}$ (A) = 1.6871ν −2.099 (mV $s^{-1})^{1/2}$, ($R^2$ = 0.9942),
(ii) $I_{pc}$ (A) = −1.7078ν −3.572 (mV $s^{-1})^{1/2}$ , ($R^2$ = 0.9946),
(iii) $I_{pa}$ (A) = 2.767ν −5.9153 (mV $s^{-1})^{1/2}$, ($R^2$ = 0.998) and
(iv) $I_{pc}$ (A) =−1.6681ν −1.9275 (mV $s^{-1})^{1/2}$, ($R^2$ = 0.9954).

Hence, these results indicate that the electrochemical kinetics is diffusion-controlled and it also can be ideal for quantitative analysis in practical applications. The CV was recorded for different glucose concentration at 50 mV $s^{-1}$ in 0.2 M NaOH solution (Fig. S3, SI). The studies show that synergistic effect of $Co_3O_4$ NPs and MWCNT were effectively electro catalyse the direct glucose oxidation.

Since cyclic voltammetry has the limitations to the low concentration measurements, chronoamperometry responses were investigated to detect the glucose. The chronoamperometry was executed by successive addition of 50 μM glucose into 10 mL of 0.2 M NaOH solution at constant intervals. To investigate the best optimal applied potential, chronoamperometry was carried out at different applied potentials such as 0.5, 0.55 and 0.6 V to yield the excellent electrochemical properties (Fig. 4a). From these results, it is seen that the signal-to-background ratio increases with the potential range from 0.5 to 0.6 V and observe that current response recorded for the 0.55 V is greater than the other applied potentials and which is supported from the CV results, where ~0.55 V the glucose oxidation peak potential was observed. Hence, 0.55 V was chosen as an optimal applied potential for the further chronoamperometry investigation. Using these optimal conditions, the chronoamperometry of the modified GCE electrodes was examined. From the Fig. 4b it can be seen that current response recorded for $Co_3O_4$/MWCNT/GCE (curve a) is 40% greater than the $Co_3O_4$/GCE (curve b) with the incremental addition of glucose (50 μM) and reaches the 95% of the steady-state current within 5 s (Fig. 4c) indicating the $Co_3O_4$/MWCNT nanocomposites efficiently catalyse the oxidation of glucose. The calibration curve for the electrochemical responses of the $Co_3O_4$/MWCNT/GCE electrode to glucose concentration is shown in Fig. 4d. From the slope of the calibration curve, the sensitivity of the sensor was found to be 5089.1 μA $mM^{-1}cm^{-2}$ for a linear glucose concentration range from 0.05 mM to 12 mM with a linear coefficient of $R^2$ = 0.988. The limit of detection (LOD) is determined using the Eqs. 4 and 5.

$$Sensitivity = slope\ of\ the\ calibration\ curve \quad \ldots (4)$$

$$LOD = \frac{3.3*\sigma}{slope} \quad \ldots\ldots\ldots\ldots (5)$$

Where, $\sigma$ is the standard deviation of the slope. From the calculations, the LOD was of the sensor was found to be 10.42 μM. The sensors were also compared with the previously reported nanomaterial based enzyme-free glucose sensors and are as shown in Table 1. As it can be seen from the table, the fabricated sensor shows highly enhanced sensitivity and LOD due to the excellent catalytic activity of $Co_3O_4$ -NPs and the electrical network formed through self-assembled $Co_3O_4$-NPs distributing on the surface of MWCNT, which not only can keep their intrinsic excellent electrical conductivity but also facilitates easy access of $Co_3O_4$ NPs to glucose oxidation. Therefore, the direct electrochemical glucose oxidation can be greatly enhanced with the use of $Co_3O_4$/MWCNT composites.

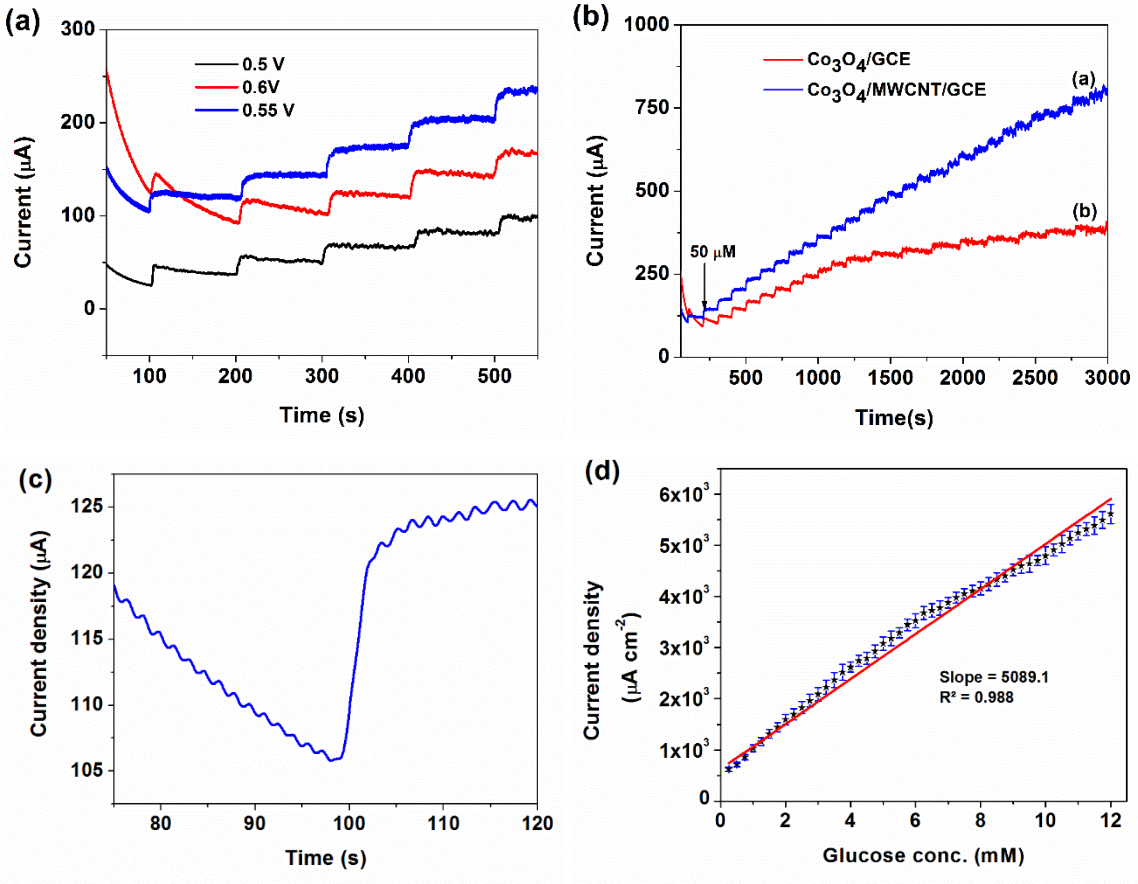


**Fig. 4**. (a) Amperometric responses of $Co_3O_4$/MWCNT/GCE at different potentials in 0.2 M NaOH with a dropwise addition of 50 μM glucose at every 50 s, (b) Current–time responses at 0.55 V with an increasing glucose concentration (50 μM) per 100 s for $Co_3O_4$/MWCNT/GCE electrode, (c) Response time measurement using i-t curve and (d) The current density response vs. glucose concentration at $Co_3O_4$/MWCNT/GCE electrode.

Table 1. Comparison of non-enzymatic glucose sensing performance based on different electrode materials of transition metal compounds.

| Electrode | Sensitivity (μA $mM^{-1}$ $cm^{-2}$) | Linear range (up to, mM) | LOD (μM) | Applied Potential (V) | Response Time (s) | Ref. |
|---|---|---|---|---|---|---|
| $Co_3O_4$ nanofibers | 36.25 | 2.04 | 0.97 | +0.60 | 7 | [19] |
| CuO nanospheres | 404.53 | 2.6 | 1.0 | +0.60 | - | [41] |
| Ni NPs -CNF paste lectrode | 420.4 | 2.5 | 1.0 | +0.55 | 5 | [42] |
| CuO nanofibers | 431.3 | 2.5 | 0.8 | +0.40 | 1 | [43] |
| SA-CNT thin films with Cu Nps electrode | 602.0 | 1.8 | 0.1 | +0.60 | - | [34] |
| Ni nanowire arrays (NiNWAs) | 1043 | 7.0 | 0.1 | +0.55 | - | [44] |
| CuxO flowers | 1620 | 6.0 | 49 | +0.50 | - | [45] |
| CuO–MWCNTs array electrode | 2190 | 3.0 | 0.8 | +0.55 | 2 | [46] |
| $IrO_2$/ $PbO_2$-carbon microelectrodes | - | 20 | 50 | +0.75 | 0.5 | [47] |
| Self-assembled $Co_3O_4$-MWCNT /GCE | **5089.1** | **12** | **10.42** | **+0.55** | **3** | **Present work** |

Journal Name

ARTICLE

**Effect of interfering species, stability and Reproducibility**

The biomolecules like fructose, sucrose, maltose, AA, DA and UA are potentially interfering ions with human blood glucose and these may also get easily oxidized at the applied potential on the sensor electrode. Hence these interference biomolecules were also tested amperometrically at +0.55 V along with glucose on the $Co_3O_4$/MWCNT/GCE in 0.2 M NaOH solution (Fig. 5). From the Fig. 5 it can be seen that response obtained for 2 mM concentration of Fructose, maltose, sucrose, AA, DA and UA were less than 3% of that obtained for 2 mM glucose which indicates the remarkable selectivity of the sensor for glucose detection in the presence of common interference electro active molecules.

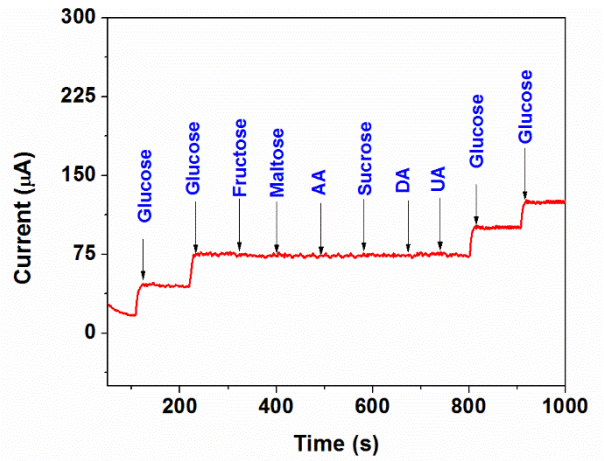


Fig. 5 Interference test of the sensor in 0.2 M NaOH at +0.55 V with 2 mM glucose and other interferons as indicated.

Long term stability experiments were investigated to evaluate the performance of the $Co_3O_4$/MWCNT/GCE enzyme-free sensor, as shown in Fig. 6a. The sensor shows the current response to glucose over a period of three weeks (five identical electrodes) during which 85% current retained was observed. However, when sensor was not in use it was stored at lab atmosphere. These results suggest that the $Co_3O_4$/MWCNT/GCE electrode possessed a good stability. The reproducibility was examined for ten identically constructed electrodes at 50 μM of glucose concentration shows 4.1% of relative standard deviation (RSD) suggesting excellent reproducibility (Fig. 6b). From these results, it may be confirmed that the $Co_3O_4$/MWCNT/GCE electrode has a greater stability and reproducibility that makes it applicable for practical use.

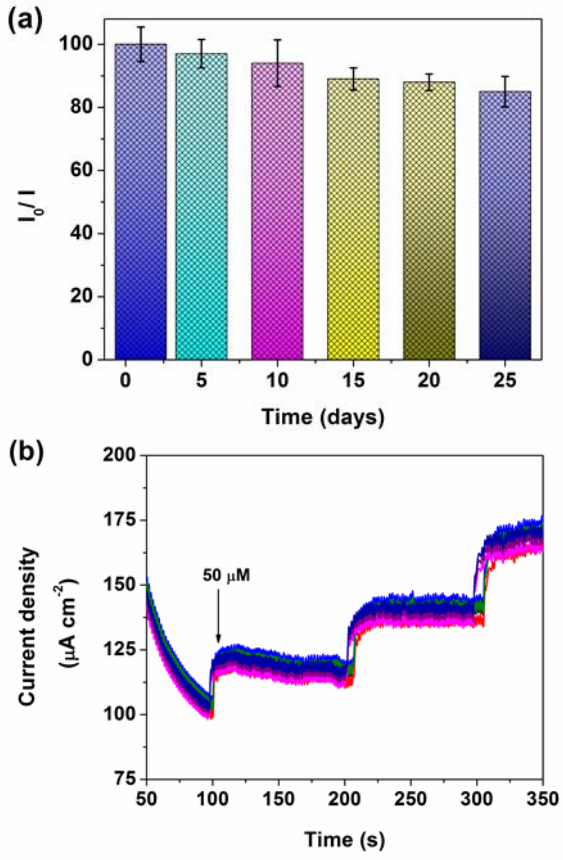


Fig.6. (a) Stability of the sensor stored at ambient conditions over three weeks using 0.2 M NaOH with 2.0 mM glucose at +0.55 V and (b) i-t response for stability check using ten identical $Co_3O_4$/MWCNT/GC electrodes.

Finally, as a real application, the $Co_3O_4$/MWCNT/GCE was applied to the determination glucose concentration in human blood plasma samples. Blood plasma samples without any pre-treatments were injected into 5 mL of 0.2 M NaOH at an applied potential of +0.55 V. The measured current change was correlated with the

glucose concentration according to the calibration curve in Fig. 4d and then compared with the value obtained using a commercial glucose meter (Free Style Freedom Lite Glucose Monitoring System, Abbott Diabetes Care) as shown in the table 2. The results show that recovery of the samples are > 94 % with the relative standard deviation (RSD) less than 7 %. Hence, these results suggest that, the $Co_3O_4$/MWCNT/GCE composite, a potential material for the fabrication of enzyme-free glucose sensors.

Table 2. The detection of glucose in human blood plasma samples

| Sample | Glucose (mM) | RSD (N = 5) | Glucose (mM) (Commercial glucose meter) | Recovery (%) |
|---|---|---|---|---|
| 1 | 6.1 | 4.4 % | 6.3 | 96.4 |
| 2 | 4.6 | 3.8 % | 4.9 | 94.2 |
| 3 | 4.5 | 5.2 % | 4.6 | 96.4 |
| 4 | 5.1 | 3.7% | 5.2 | 97.6 |

## Conclusions

Self-assembled uniformly decorated cobalt oxide nanoparticles decorated multi-walled carbon nanotubes were successfully synthesized by simple wet chemical sol-gel method. The synthesized composite was employed to fabricate enzyme-free glucose sensor for the detection of glucose. The results of cyclic voltammetry, chronoamperometry revealed that uniformly dispersed cobalt oxide on multi-walled carbon nanotubes possessed attractive electrochemical properties such as high sensitivity, low detection of limit, high selectivity, greater stability and excellent reproducibility. These improved performances are ascribed to the synergistic effect of cobalt oxide and multi-walled carbon nanotubes. Thus, the cobalt oxide-multi-walled carbon nanotubes nanocomposite is expected to be promising materials for the fabrication enzyme-free glucose sensors.

## Acknowledgements

The authors are thankful to CeNSE, Indian Institute of Science, Bangalore for providing analytical services and NITK, Surathkal, India, for providing necessary laboratory facilities.

**Notes**

[a]Department of Chemistry, National Institute of Technology Karnataka, Surathkal, Srinivasnagar-575025, India
* e-mail: ram@nitk.edu.in, brchandra@gmail.com

**References**

1. J. Wang, *Electroanalysis,* 2005*,* **17**, 7–14.
2. H. Jiang, *Small,* 2011*,* **7**, 2413–2427.
3. M. Gao, L. Dai and G. G. Wallace, *Electroanalysis,* 2003*,* **15,** 1089–1094.
4. T. Zhu, B. Xia, L. Zhou and X. W. (David) Lou, *J. Mater. Chem.,* 2012*,* **22**, 7851–7855.
5. Z. Dong, C. Zhou, H. Cheng, Y. Zhao, C. Hu, N. Chen, Z. Zhang, H. Luo and L. Qu, *Carbon,* 2013, **64***,* 507–515.
6. N. G. Tsierkezos, U. Ritter, N. Wetzold and A. C. Hübler, *Microchim. Acta,* 2012*,* **179**, 157–161.
7. C. Lu, W. Liu, H. Li and B. K. Tay, *Chem. Commun.,* 2014*,* **50,** 3338–3340.
8. P. H. Jampani, O. Velikokhatnyi, K. Kadakia, D. H. Hong, S. S. Damle, J. A. Poston, A. Manivannan and P. N. Kumta, *J. Mater. Chem. A,* 2015*,* **3**, 8413–8432.
9 R. Prasad, N. Gorjizadeh, R. Rajarao, V. Sahajwalla and B. R. Bhat, *RSC Adv.,* 2015, **5**, 44792–44799.
10 R. Prasad and B. R. Bhat, *Sens. Actuators B Chem.,* 2015, **220,** 81–90.
11. F. Sun, L. Li, P. Liu and Y. Lian, *Electroanalysis,* 2011*,* **23**, 395–401.
12. H. Yu, X. Jian, J. Jin, X. Zheng, R. Liu and G. Qi, *Microchim. Acta,* 2014*,* **182**, 157–165.
13. X.-C. Dong, H. Xu, X.-W. Wang, Y.-X. Huang, M. B. Chan-Park, H. Zhang, L.-H. Wang, W. Huang and P. Chen, *ACS Nano,* 2012*,* **6**, 3206–3213.
14. X. Wang, X. Dong, Y. Wen, C. Li, Q. Xiong and P. Chen, *Chem. Commun.,* 2012, **48**, 6490–6492.
15. L. Zhang, S. Yuan, L. Yang, Z. Fang and G. Zhao, *Microchim. Acta,* 2013, **180**, 627–633.
16. J. Yuan, Y. Cen, X.-J. Kong, S. Wu, C.-L. Liu, R.-Q. Yu and X. Chu, *ACS Appl. Mater. Interfaces,* 2015, **7 (19)**, 10548–10555
17. J. Lang, X. Yan and Q. Xue, *J. Power Sources,* 2011*,* **196**, 7841–7846.

18. S. G. Kandalkar, J. L. Gunjakar and C. D. Lokhande, *Appl. Surf. Sci.,* 2008, **254**, 5540–5544.
19. Y. Ding, Y. Wang, L. Su, M. Bellagamba, H. Zhang and Y. Lei, *Biosens. Bioelectron.,* 2010*,* **26**, 542–548.
20. C.-W. Kung, C.-Y. Lin, Y.-H. Lai, R. Vittal and K.-C. Ho, *Biosens. Bioelectron.,* 2011, **27***,* 125–131.
21. S. Yang, G. Cui, S. Pang, Q. Cao, U. Kolb, X. Feng, J. Maier and K. Müllen, *ChemSusChem,* 2010*,* **3***,* 236–239.
22. W. Y. Li, L. N. Xu and J. Chen, *Adv. Funct. Mater.,* 2005, **15**, 851–857.
23. Z. Meng, B. Liu, J. Zheng, Q. Sheng and H. Zhang, *Microchim. Acta,* 2011*,* **175**, 251–257.
24. G. Wang, X. Shen, J. Yao, D. Wexler and J. Ahn, *Electrochem. Commun.,* 2009*,* **11**, 546–549.
25. A. Tavasoli, K. Sadagiani, F. Khorashe, A. A. Seifkordi, A. A. Rohani and A. Nakhaeipour, *Fuel Process. Technol.* 2008*,* **89**, 491–498.
26. L. Fu, Z. Liu, Y. Liu, B. Han, P. Hu, L. Cao and D. Zhu, *Adv. Mater.* 2005*,* **17***,* 217–221.
27. A. Heller and B. Feldman, *Chem. Rev.,* 2008*,* **108**, 2482–2505.
28. D. Chirizzi, M. R. Guascito, C. Malitesta and E. Mazzotta, in Sens. Microsyst. (Eds.: G. Neri, N. Donato, A. d' Amico, C.D. Natale), *Springer Netherlands*, 2011, pp. 339–343.
29. A. Badia, R. Carlini, A. Fernandez, F. Battaglini, S. R. Mikkelsen and A. M. English, *J. Am. Chem. Soc.,* 1993*,* **115,** 7053–7060.
30. C. Malitesta, F. Palmisano, L. Torsi and P. G. Zambonin, *Anal. Chem.,* 1990*,* **62**, 2735–2740.
31. M. Wooten, S. Karra, M. Zhang and W. Gorski, *Anal. Chem.,* 2014, **86**, 752–757.
32. R. Wilson and A. P. F. Turner, *Biosens. Bioelectron.,* 1992*,* **7**, 165–185.
33. X. Kang, Z. Mai, X. Zou, P. Cai and J. Mo, *Anal. Biochem.,* 2007*,* **363**, 143–150.
34. X. Li, Q. Zhu, S. Tong, W. Wang and W. Song, *Sens. Actuators B Chem.,* 2009, **136***,* 444–450.
35. Z. H. Ibupoto, K. Khun, V. Beni, X. Liu and M. Willander, *Sensors,* 2013*,* **13**, 7926–7938.
36. S. Park, H. Boo and T. D. Chung, *Anal. Chim. Acta,* 2006, **556**, 46–57.
37. R. Rajarao and B. R. Bhat, *Synth. React. Inorg. Met.-Org. Nano-Met. Chem.,* 2013*,* **43***,* 1418–1422.
38. J. Wu, Y. Xue, X. Yan, W. Yan, Q. Cheng and Y. Xie, *Nano Res.,* 2012*,* **5***,* 521–530.
39. D. Jung, M. Han and G. S. Lee, *Sens. Actuators B Chem.,* 2014*,* **204**, 596–601.
40. N. Yan, L. Hu, Y. Li, Y. Wang, H. Zhong, X. Hu, X. Kong and Q. Chen, *J. Phys. Chem. C,* 2012*,* **116**, 7227–7235.
41. E. Reitz, W. Jia, M. Gentile, Y. Wang and Y. Lei, *Electroanalysis,* 2008*,* **20**, 2482–2486.
42. Y. Liu, H. Teng, H. Hou and T. You, *Biosens. Bioelectron.,* 2009, **24**, 3329–3334.
43. W. Wang, L. Zhang, S. Tong, X. Li and W. Song, *Biosens. Bioelectron., 2009,* **25**, 708–714.
44. L.-M. Lu, L. Zhang, F.-L. Qu, H.-X. Lu, X.-B. Zhang, Z.-S. Wu, S.-Y. Huan, Q.-A. Wang, G.-L. Shen and R.-Q. Yu, *Biosens. Bioelectron*., 2009*,* ***25***, 218–223.
45. C. Li, Y. Su, S. Zhang, X. Lv, H. Xia and Y. Wang, *Biosens. Bioelectron.,* 2010*,* **26**, 903–907.
46. J. Yang, L.-C. Jiang, W.-D. Zhang and S. Gunasekaran, *Talanta,* 2010*,* **82**, 25–33.
47. W. Gorski and R. T. Kennedy, *J. Electroanal. Chem*., 1997**, 424,** 43–48.

Table of content

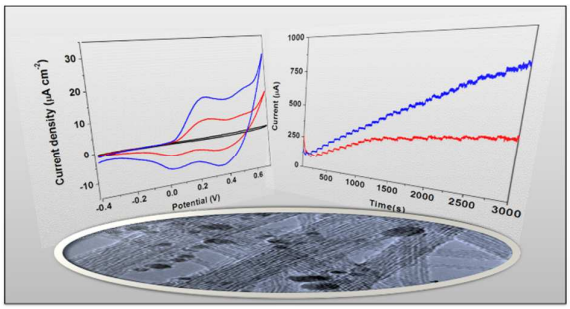


Electrochemical detection and sensing of glucose by direct glucose oxidation using non-enzymatic sensor with high efficiency and greater stability.

**Table of content**